OPTICAL NAVIGATION TO A NEAR EARTH OBJECT

Stéphanie Delavault[1], Jérôme Berthier[2], Jacques Foliard[1]

[1]CNES, 18, av. E. Belin - 31401 Toulouse Cedex 9 - France, Stéphanie.Delavault@cnes.fr - Jacques.Foliard@cnes.fr
[2]IMCCE, , 77 av. Denfert Rochereau - 75014 Paris - France, Jerome.Berthier@imcce.fr

ABSTRACT

In the framework of the research and technology program at CNES, an ongoing joined study with IMCCE allows to simulate and analyse the astrometrical process of optical navigation during interplanetary trajectory. The main objective is to identify the accuracy of optical data, including the errors due to the entire process, in order to estimate the orbit determination performance of a mission such as an interplanetary transfer toward a Near Earth Object. Thus a planetary scene viewer has been developed which allows to simulate pictures of planets or asteroids in front of a star background taken by an on-board camera. Using this tool it is so possible to simulate real optical data, and also to evaluate their accuracy. Then these results are applied in a very preliminary mission analysis of a transfer toward a near Earth asteroid.

ACRONYMS

CNES	Centre National d'Etudes Spatiales
IMCCE	Institut de Mécanique céleste et de Calcul des Ephémérides
NEO	Nearth Earth Object
OD	Orbit Determination
PSF	Point Spread Function

1. INTRODUCTION

This study has been performed in the context of the CNES research and technology program in collaboration with IMCCE (Institut de Mécanique Céleste et de Calcul des Ephémérides). It deals with interplanetary navigation towards Near-Earth Objects using optical data.
Optical navigation performance have previously been studied at CNES, mainly for Mars approach phase (see [1]), but also for Earth to Mars transfer (see [2]). The purpose of the present study is to better understand the general process of data generation in order to be able to use consistent assumptions for mission analysis in term of model errors.
The first part details an analysis of the astrometrical process performed by IMCCE. A planetary scene viewer has been developed which allows to simulate pictures of planets or asteroids in front of a star background taken by an on-board camera. This tool takes into account the probe trajectory, the planetary ephemeris and the stars locations based on an astrometrical catalogue, but also the surface properties of the bodies to compute the light-scattering and the phase angle. Then this realistic view is filtered through an optical instrumentation process that considers the optical properties of the camera and the computed magnitudes of the bodies to produce a photometric picture of the view. Examples of views before and after the camera filtering are given. The astrometrical process applied to the picture is then described. It allows to extract the position of the photocentre of the observed body, and then its centre of gravity. The other part of this study consists in the evaluation of the accuracy of the produced data, due to the performance of the camera or to the astrometrical process itself, for example the estimation of the accuracy of the shift between the photocentre and the centre of gravity is described.
In the second part, the results of the previous analysis are applied to an interplanetary trajectory in the framework of a mission towards a Near Earth Object. The mission aims at landing on an asteroid which trajectory crosses the Earth orbit. Some criteria for the asteroid selection for optical navigation needs are given. The preliminary navigation performance study using CNES orbit determination covariance analysis tool (EPERON) is finally detailed in order to estimated the trajectory determination accuracy.

2. ASTROMETRICAL PROCESS

2.1 Planetary Scene Viewer

In order to study the astrometrical aspect of optical navigation, IMCCE developed a planetary scene viewer to simulate pictures of an on-board camera. This tool provides a realistic scene of a planetary system or an asteroid in front of a star background taking into account the probe trajectory, the planetary ephemeris and the stars locations (see Figure 1 and Figure 2 : Output and associated data of the planetary scene viewer showing a perfect view of the Mars system ; the point marked 'P' represents Phobos as seen from a spacecraft on the way to Mars. The background displays stars until magnitude 14). The orientation of the target in relation with the probe is computed in a true apparent frame of the date using planetary theories such as VSOP87 [3] or DE405 [4] for the planets, specific dynamical solutions for natural satellites and numerical

integration of the n-body problem for asteroids. The apparent aspect of the target is computed using standard definitions of planetary rotation [5] and physical parameters recommended by IAU. When it exists, a topographic model represents the target and a true map is used to wrap up the object. The background of the scene is made up of stars that comes from any stellar catalogue (UCAC, TYCHO, USNO-A or B, etc.).

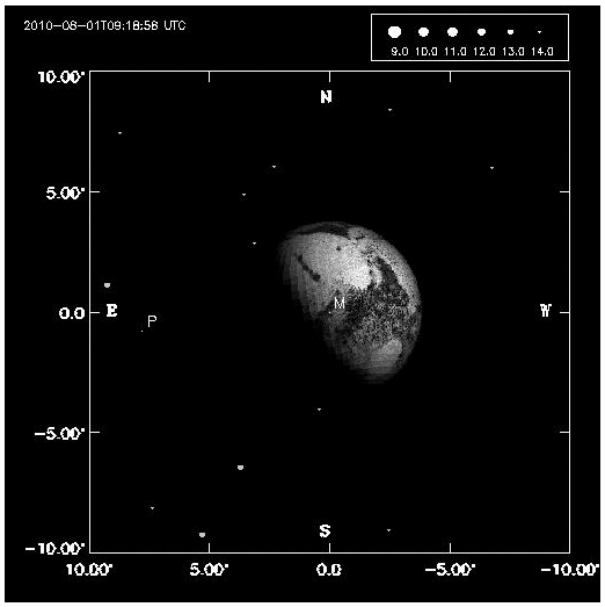

Figure 1 - Output of the Planetary Scene Viewer, without PSF

Scene specification	
* Date:	2010-08-01T09:18:58 UTC
* Frame:	512 x 512 pixels
* Scale:	2.344 arcsec/px 3.520E+01 km/px
* Frame center:	Mars:RES_MP_2009_IMCCE

Mars	Phobos
SEP: 292.23 / -7.35 SSP: 222.81 / 19.99 NP: 10.87 deg Dg: 2.059557390E-02 au Phase: 73.51 deg App. radius: 3.790 ' Visual Mag: -7.76 Alb. Geom.: 0.015 Scat. law: Hapke Photocenter shift : pX = -89.186 arcsec pY = 61.222 arcsec	SEP: 130.55 / -7.35 SSP: 60.98 / 18.98 NP: 12.07 deg Dg: 2.055555662E-02 au Phase: 73.39 deg App. radius: 0.871 " Visual Mag: 6.72 Alb. Geom.: 0.005 Scat. law: Hapke Photocenter shift : pX = 3.118 arcsec pY = -0.141 arcsec Relative position : Phobos/Mars X = 7.793 arcmin Y = -0.772 arcmin

Figure 2 - Data displayed by the planetary scene viewer

The image of a celestial body which is formed on the focal plane of an on-board telescope is spread out by the diffraction linked to the telescope. This degradation can be modelled by a convolution between the real image and a function, called point spread function (PSF), appropriated for the optical system: it represents its impulse response. In the case of a telescope with a circular pupil and in the absence of atmosphere, the impulse response is a diffuse circular disc known as Airy's disc surrounded by much fainter concentric circular rings. As the light coming from the object can be considered parallel and monochromatic, and as the image plane is at a distance large compared to the size of the object, one can apply the theory of the Fraunhofer diffraction to compute the PSF. The theoretical resolution of the telescope is then given, for a wavelength λ, by the ratio λ/D where D is the size of the pupil. As a consequence, the more one increases the size of the pupil, the more one improves the resolution of the telescope and thus its ability to see fine details. To take into account this effect, the perfect view of the planetary system generated by the scene viewer is convolved by a theoretical PSF that considers the optical properties of the camera (see Figure 3 : the perfect view showed in Figure 1 has been convolved by a PSF corresponding to a 8cm pupil and 5 µm wavelength telescope).

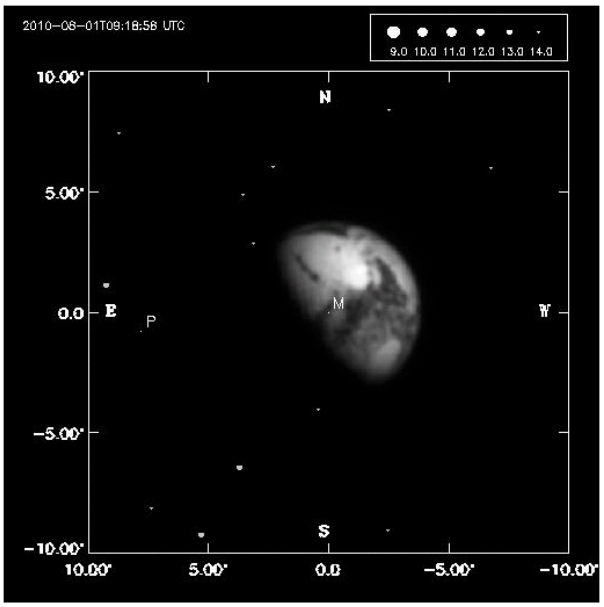

Figure 3 - Output of the planetary scene Viewer, with PSF

2.2 Astrometrical process

The image generated by the planetary scene viewer is analysed to measure the astrometrical positions of the planetary target with respect to the astrometrical star background in order to select targets suitable for navigation and to estimate the orbit determination performance.

The positions of the targets on the image are measured by centroiding with a two-dimensional Moffat-Gauss profile. If necessary, the background is modelled by an inclined quadratic surface to avoid strong luminosity gradient in the vicinity of bright targets. That ensures the photometric positions to be measured at a level of few tenth of pixels. The astrometrical parameters (scale and orientation factors) which allow to transform the

plate (x,y) coordinates into celestial coordinates are computed using a classical plate constants model customized to take into account only effects that can't be modelled *a priori* [6]. The connecting function between the image plane and the sky is thus determined by a fit between the observed (i.e on the image plane) and the computed (i.e. ephemeris calculation) positions of the astrometrical reference stars. Then the position of the planetary target is achieved in relation to the position of the probe at the time of the recorded image in the apparent framework of the spacecraft. Thinking that the heliocentric position of the planetary target is well known, one can infer the geometric position of the probe in the solar system by two angles in an ecliptic reference frame. This implies the inversion of the transformations taken into account in the astrometrical reduction process (such as light aberrations, precession and change of reference frame because astrometrical catalogue as expressed in a barycentric equatorial frame) and the correction of all physical effects that can affect the trajectory of the probe (non-gravitational effect such as solar wind or Yarkowski effect, ...). Finally, we trust our astrometry at a level of a few tenth of milli-arcseconds depending on the accuracy of reference star positions, frame transformation and other effects not yet discussed.

2.3 Errors

The accuracy of the astrometrical position of a target in an image depends mainly on the observational errors on the target and the reference stars, on the catalogue error of the reference stars and on the model of the astrometrical reduction (i.e. the form of the connecting function between the image and the sky). The total, single-image, external error e_t of the position of an object near the centre of an image can be estimated by [7]:

$$e_t^{\,2} = \frac{e_c^{\,2} + (S \cdot e_r)^2}{n-m} + (S \cdot e_o)^2$$

where e_c is the mean catalogue error of the reference stars (in arcsec), e_r is the mean total observational error of the reference stars, including image errors and night errors (in pixel) and e_o is the total observational error of object (in pixel) ; S is the scale factor of the image (arcsec/pixel), n is the number of reference stars used in the plate solution and m is the number of degrees of freedom (i.e. the number of constants determined in the plate solution). This relation allows one to estimate, for a type of receptor (defined by its scale factor) and an astrometrical catalogue, the maximu m accuracy that one can expect after an astrometrical reduction process (cf. Table 1).

n-m	USNO ($e_c = 0".5$)	UCAC-2 ($e_c = 0".025$)
1	0".574	0".284
2	0".430	0".246
5	0".313	0".219
10	0".263	0".210
20	0".233	0".205

Table 1 - Accuracy expected for different values of n-m; we suppose a scale factor equal to 2 arcsec/px (~10 µrad/px) and a total observational error on the target and reference stars equal to 0.1 pixel (i.e. 0.2 arcsec or 1 µrad)

As shown in Table 1, the lack of accuracy of the catalogue of reference stars can be recovered by a large set of reference stars in the reduction process. But, in any case, the accuracy of the result is limited by the total observational error of object (e_o).

Another kind of error can degrade the astrometric solution: when the target is a solar system object and when it is resolved in the image, the photocentre (i.e. the photometric position as measured on the image) and the centre of mass of the target do not coincide. It implies an additional error on the target astrometrical position which could be not negligible. It's all more true since the phase angle of the solar system objects as seen from a spacecraft can be large (i.e. > 30 degrees).

The computation of the offset of the photocentre compared to the centre of mass of a spherical object of radius R observed under a phase angle α is obtained analytically for some simple light-scattering laws. In the case of a dark object, such as an asteroid or a planetary satellite, suitable light-scattering models are the Minnaert's law (function of the limb darkening parameter k) or the Lommel-Seeliger's law. Only the second one authorises an analytical expression of the photocentre offset for an unspecified phase angle [8]:

$$d_{L-S} = \frac{2R}{3p} \cdot \frac{\sin a + (p - a) \cdot \cos a}{\cot\frac{a}{2} - \sin\frac{a}{2} \cdot \ln\left(\cot\frac{a}{2}\right)}$$

We have successfully applied this law to model the photocentre offset of the dark and irregular shape of Phobos during a simulated space mission toward Mars (generic orbit). The photocentre offset is calculated on the images generated by the planetary scene viewer using a Minnaert's law (k =0.55) and the topographic model of Phobos. On the whole mission, it achieves a

maximum of about 6-km that is about half the equivalent radius of Phobos. The comparison with the Lommel-Seeliger's law shows residuals with a mean deviation of about 100-m with a standard deviation of about 400-m. It corresponds to the non-spherically of Phobos. Thus, as the role of the light-scattering model is small (order of one percent of the offset size) [8], the use of the Lommel-Seeliger's law is suitable for modelling the photocentre offset of the targets.

3. OPTICAL NAVIGATION TO A NEO

The principal interest of optical navigation for interplanetary missions is that it provides uniform angular information on 2 dimensions and, in particular, out of the plane of the orbit of the probe. It is thus complementary to the classical navigation technique for which information is basically on one dimension (measurement of distance, Doppler).
Among the space exploration challenges, delivering a spacecraft to an asteroid is a typical objective for future exploration missions. In a navigation point of view, this kind of mission is a good candidate for the use of optical measurements during the cruise phase mainly due to its cost-effectiveness, since the navigation tasks of the ground segment are quite reduced.

3.1 Mission Overview

In the context of the research program at CNES, some perspective of missions toward near Earth asteroids are considered. The aim of such a mission would be to land on an asteroid to analyse its soil and structure. Asteroids crossing the Earth orbits would be privileged targets as they would be easier to reach than farther ones. During the cruise phase, it is also envisaged to make swing-byes of intermediate targets to take pictures. As this mission is still in a very preliminary state, only general assumptions have been made for this study. The Figure 4 illustrates a basic transfer orbit from Earth toward a NEO.

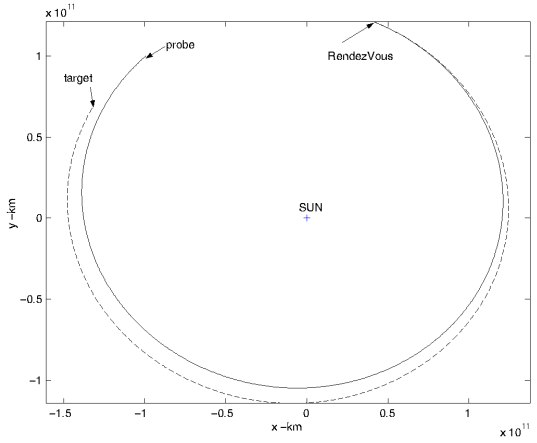

Figure 4 - Trajectory toward the targeted NEO

3.2 Selection of the asteroids

The first step of this study was to select asteroids usable for optical navigation during the cruise phase. The criteria used for this selection have been deduced from the capability of the camera to image correctly the target thus producing a picture of enough good quality to be used by the astrometrical process. Typical characteristics of the on-board camera are displayed in the Table 2. These data give the bases of the definition of some selection criteria. In addition to characteristics inherent to the body, such as absolute magnitude and albedo parameter, the visual magnitude depends on the Sun-body and probe-body distances and on the phase angle (see [2]). The observed body would be as much identifiable on the camera CCD as it is close to the probe (but not to close, in order not to be considered as a resolved body for the astrometrical process) and well lighted by the Sun. Another selection criteria is the relative probe-body velocity : if the asteroid moves to fast in the probe plane of sky with respect to the dynamic range of the camera, this would induce a spread on the picture that would imply a less accurate astrometrical reduction. Other aspects such as the star background can be considered, but they do not have been taken into account in this study. Table 3 presents the criteria and associated thresholds used for this selection.

Characteristics	Values
Pixel size	10 µrad
Field of view	1 deg²
Maximal magnitude	12

Table 2 - Camera Characteristics

Criteria for selection	Thresholds
Distance	≤ 100 millions km
Phase angle	≤ 40°
Relative velocity	≤ 7 km/s

Table 3 - Criteria for asteroids selection

The following graphs present the criteria repartition over the cruise phase of the mission : for each date, the criteria associated to the selected asteroids are plotted. Some asteroids could be kept in the selection from one date to another. These graphs show that depending on the date in the mission, the number of selected bodies varies from 2 to 14.

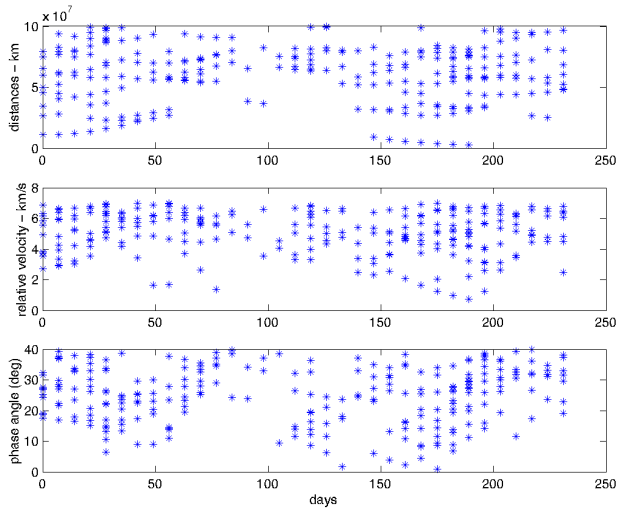

Figure 5 - Selection criteria

It could also be noted in these graphs, that the asteroid giving the lowest distance and the lowest relative velocity is the target of the mission. This asteroid has been rejected after the 200th day because of its phase angle that overcomes the associated threshold.

3.3 Orbit determination performance

A covariance analysis of the orbit determination performance have been done using CNES tool EPERON (see [9]). This analysis allows to use the assumptions defined by the IMCCE for the astrometrical model errors and the asteroids selection method. The aim of such kind of studies is basically to determine if the mission would be feasible in a navigation point of view using only optical data and at which rate, in order to reach the targeted body with the required accuracy. As the mission is not completely defined, the present analysis only aimed at testing the process and better understanding the resulting OD performance.

The tracking schedule considers only optical data : every seven days, a session of pictures of selected asteroids is performed. Each asteroid is imaged only once per session. This leads to roughly 90 asteroids imaged during the entire cruise phase. Practically, this is a challenging operation, because it implies to perform observation campaigns on these asteroids previously to the mission to get the most accurate ephemerides as possible. After such a campaign, the reachable accuracy is roughly of 50 milli-arseconds (with respect to the Earth), which has been approximately translated into 100 km of absolute error on the ephemerides of the asteroids. Table 4 summarises the error assumptions used for the covariance analysis.
The analysis of part 2 mainly deals with resolved bodies (such as planets or natural satellites in approach phases). However, in cruise phase the imaged asteroids would most probably be non resolved bodies. The expected astrometrical error in such cases is about 0.1 pixel. For this study, a worst case value has been used.

Source	1-σ a priori uncertainty	
Data noise	2.4 µrad	-
Probe ephemeris	~Infinite	estimated
Asteroid ephemeris	100 km	considered
Photocentre shift	400 m	considered

Table 4 - Error sources

Figure 6 shows the *a posteriori* uncertainty of the probe position in the orbital local frame deduced from the covariance analysis during the cruise phase. It can be noted from this graph that the on-orbit uncertainty associated to the chosen assumptions is about a few hundredth of kilometres. This will of course have to be refined in further studies. It is also interesting to note the evolution of the error along the cruise phase. The increase about the 75th day coincides with a phase when only few asteroids have been selected for navigation (see Figure 5), leading so to less data to improve the on-orbit accuracy. According to the tracking schedule, after the 150th day of cruise, more asteroids are selected, but as noted in part 3.2 the pictures of the target that are included in the schedule seem not to be very suitable for navigation : its low relative velocity induces few dynamical information, and its close distance induces a strong impact of the ephemeris errors. Thus another case has been run suppressing the targeted asteroid from the tracking schedule. The results of this case are presented in Figure 7. A significant improvement of the on-orbit uncertainty is induced by this change of the tracking data. This implies that the navigation performance is very sensitive to the selection criteria. Further studies will be performed in order to analyse more precisely this sensitivity and to propose more effective criteria.
The computed uncertainty is still great at the end of the cruise phase considering the purpose of such a mission. However, it should be kept in mind that this has been obtained with only optical measurement on asteroids and under specific assumptions. The performance would probably increase with a specific tracking schedule during the approach phase, leading to locate more precisely the probe with respect to the target. Moreover, these kind of data are particularly interesting as a complement to classical range and Doppler data, as they give information in the out-of plane direction. A tracking schedule combining both types of measurement would allow to get a better accuracy.

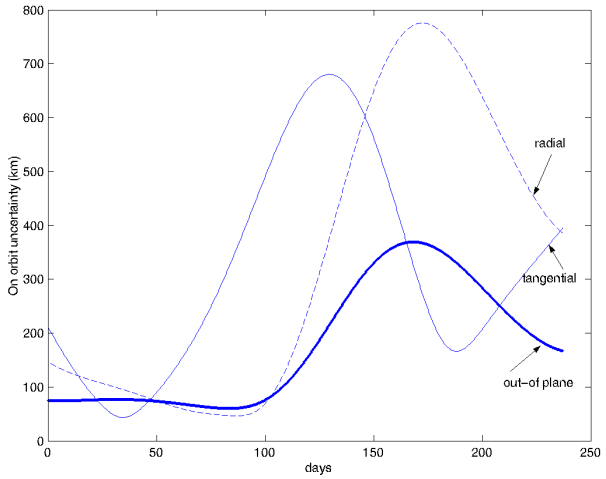

Figure 6 - On-orbit uncertainty in the Local Orbital Frame with the baseline schedule

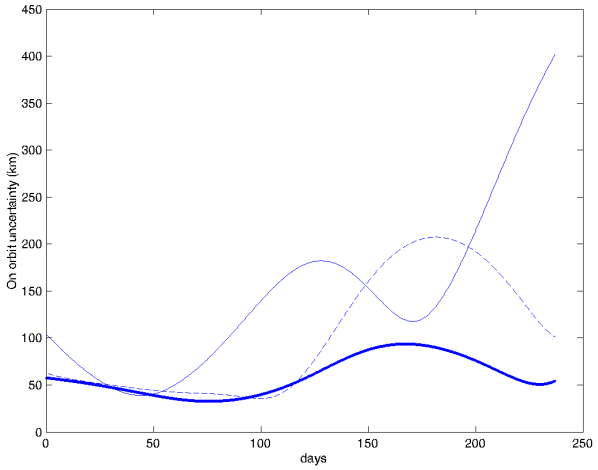

Figure 7 - On-orbit uncertainty in the Local Orbital Frame without using pictures of the target

4. CONCLUSION

This analysis of the optical navigation process and performance allows us to dispose from a planetary scene viewer simu lating pictures taken by an on-board camera during interplanetary missions. The analyses performed by IMCCE gave some information about the order of magnitude of error sources on this type of data. Some selection criteria have been applied on asteroids for navigation purpose. The preliminary orbit determination analysis based on these assumptions showed a significant sensitivity of the OD performance to the selected asteroids and thus to the selection criteria that will have to be fine tuned in further studies. This preliminary study set the basis of further OD mission analysis for interplanetary missions based on asteroid navigation.

References

1. S. Delavault, J. Foliard, *Optical Navigation for the Mars Premier 2007 Orbiter Approach Phase*, AAS/AIAA Space Flight Mechanics Meeting, San Antonio, Texas, USA, 2002

2. L. Chausson, S. Delavault, *Optical Navigation Performance during Interplanetary Cruise*, 17th ISSFD, Moscow, Russia, 2003

3. P. Bretagnon and G. Francou. *Planetary theories in rectangular and sperical variables. VSOP87 solutions.* Astron. Astrophys. 202, 1988

4. E. M. Standish. *JPL Planetary and Lunar Ephemerides, DE405/LE405*, Jet Propulsion Laboratory Interoffice Memorandum IOM 312.F-98-048, 1998

5. P. K. Seidelmann, V. K. Abalakin, M. Bursa, M. E. Davies, C. de Bergh, J. H. Lieske, J. Oberst, J. L. Simon, E. M. Standish, P. Stooke, P. C. Thomas. *Report of the IAU/IAG Working Group on Cartographic Coordinates and Rotational Elements of the Planets and Satellites*: 2000. Celestial Mechanics and Dynamical Astronomy, v. 82, Issue 1, 2002

6. A. Fienga and J. Berthier. *Principe de réduction d'images astrométriques*, Notes Scientifiques et Techniques du Bureau des longitudes S063, 1999.

7. D. Pascu and R. E. Schmidt. *Photographic positional observations of Saturn*, Astronomical Journal, v. 99 numb. 6, 1990

8. M. Kaasalainen and P. Tanga. *Photocentre offset in ultraprecise astrometry: Implications for barycentre determination and asteroid modelling*, Astron. Astrophys 416, 2004

9. S. Delavault, *Orbit Covariance Analysis for Planetary and Interplanetary Missions*, 14th AAS/AIAA Space Flight Mechanics Conference, Maui, Hawaii, USA, 2004.